Visual Neuroscience (2007), **24**, 449–457. Printed in the USA.

DOI: 10.1017/S0952523807070010

RESEARCH ARTICLES

Functional polarity of dendrites and axons of primate A1 amacrine cells

CHRISTOPHER M. DAVENPORT,[1] PETER B. DETWILER,[2] AND DENNIS M. DACEY[3]

[1]Neurobiology and Behavior Graduate Program, University of Washington, Seattle, Washington
[2]Department of Physiology and Biophysics, University of Washington, Seattle, Washington
[3]Department of Biological Structure, University of Washington, Seattle, Washington

(RECEIVED October 23, 2006; ACCEPTED December 16, 2006)

Abstract

The A1 cell is an axon-bearing amacrine cell of the primate retina with a diffusely stratified, moderately branched dendritic tree (~400 μm diameter). Axons arise from proximal dendrites forming a second concentric, larger arborization (>4 mm diameter) of thin processes with bouton-like swellings along their length. A1 cells are ON-OFF transient cells that fire a brief high frequency burst of action potentials in response to light (Stafford & Dacey, 1997). It has been hypothesized that A1 cells receive local input to their dendrites, with action potentials propagating output *via* the axons across the retina, serving a global inhibitory function. To explore this hypothesis we recorded intracellularly from A1 cells in an *in vitro* macaque monkey retina preparation. A1 cells have an antagonistic center-surround receptive field structure for the ON and OFF components of the light response. Blocking the ON pathway with L-AP4 eliminated ON center responses but not OFF center responses or ON or OFF surround responses. Blocking GABAergic inhibition with picrotoxin increased response amplitudes without affecting receptive field structure. TTX abolished action potentials, with little effect on the sub-threshold light response or basic receptive field structure. We also used multi-photon laser scanning microscopy to record light-induced calcium transients in morphologically identified dendrites and axons of A1 cells. TTX completely abolished such calcium transients in the axons but not in the dendrites. Together these results support the current model of A1 function, whereby the dendritic tree receives synaptic input that determines the center-surround receptive field; and action potentials arise in the axons, which propagate away from the dendritic field across the retina.

Keywords: Retina, Amacrine, Calcium, Receptive Field, Axon

Introduction

It is established that a number of large field amacrine cell types possess morphologically distinct dendritic and axonal components (Dacey, 1988, 1989, 1990; Famiglietti, 1992*a*, 1992*b*, 1992*c*; Volgyi et al., 2001; Witkovsky, 2004), but much less is known about the physiological significance of these anatomical structures. The A1 axon-bearing amacrine cell of the macaque monkey retina is an example of such a cell type (Fig. 1). A1 cell dendrites are thick, spiny, and highly branched (Fig. 1B), extending symmetrically ~ 200 μm from the soma and stratifying diffusely in the ON and OFF sublayers of the inner plexiform layer (IPL). Multiple (1–4) axons arise from the soma and proximal dendrites forming an arborization that extends away from the dendritic tree over 4 mm in the IPL. The axons are thin, sparsely branching, and along their length are swellings that resemble presynaptic boutons (Fig 1C; Dacey, 1989). Intracellular recordings from A1 amacrine cells, and similar amacrine cells in rabbit retina (Taylor, 1996; Volgyi et al., 2001) revealed that they depolarize transiently and fire action potentials at light onset and offset. The A1 receptive field mapped with small spots and bars is approximately the same size as its dendritic field (Stafford & Dacey, 1997) leading to the hypothesis that A1 cells receive inputs to their dendrites causing depolarization and initiation of action potentials, which then propagate down the axons and across the retina. Because their arborizations are so large, A1 cell axons collectively form a network that extensively covers the retina (estimates are as high as 1000 mm of axon/mm^2 retina) (Dacey, 1989; Wright & Vaney, 2004), suggesting that they serve a global function in visual processing.

Global retinal stimuli can effect ganglion cells when presented outside of their classical receptive fields (Kruger et al., 1975; Solomon et al., 2006; Werblin, 1972). Recently two studies specifically invoked axon-bearing amacrine cells as mediators of long-range inhibition of ganglion cells in response to global image motion. Roska and Werblin (2003) presented movies of natural images that shifted with saccade-like motion and found that this motion inhibited specific ganglion cell types whose dendrites

Address Correspondence and reprint requests to: Christopher M. Davenport, Department of Physiology and Biophysics, Box 357290, Seattle, WA 98195. E-mail: daven@u.washington.edu

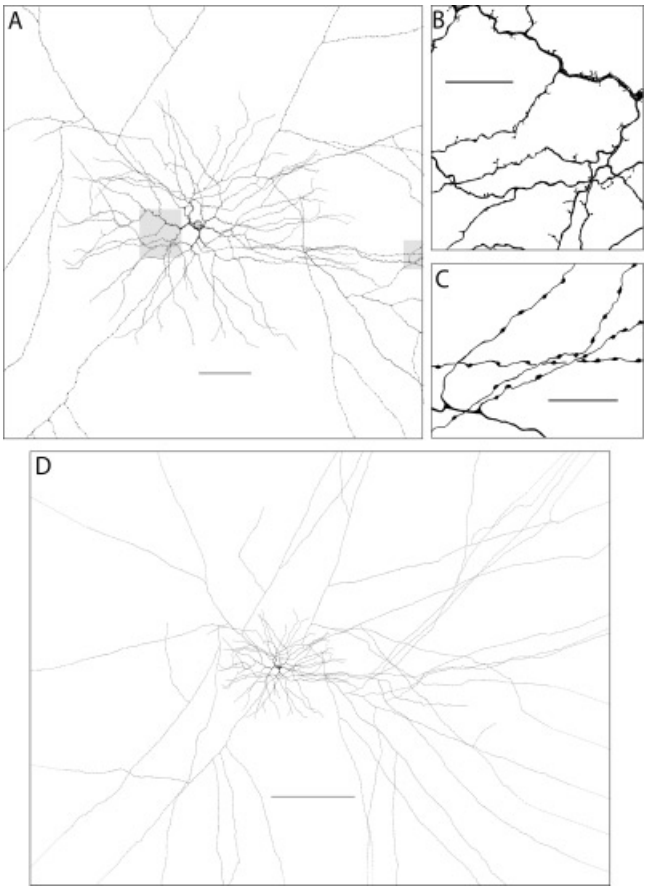

Fig. 1. A1 amacrine cell morphology. **A**: A camera lucida tracing of a Neurobiotin filled A1 amacrine cell. The dendritic tree and proximal axons can be seen. Scale bar = 100 μm. **B**: A high magnification view of the dendritic tree from the proximal shaded area in A. Dendrites are thick, spiny, and moderately branched. Scale bar = 25 μm. **C**: A high magnification view of the axonal tree from the distal shaded area in A. Axons are thin, sparsely branching, and have bouton-like swellings along their length. Scale bar = 25 μm. **D**: Low magnification image showing the axonal arbor. Scale bar = 400 μm.

stratified in the center of the IPL. They also showed that antagonists of GABA receptors and voltage-gated sodium channels could block the shift-induced inhibition, consistent with axon-bearing amacrine cell involvement. Olveczky et al. (2003) showed that a grating moved outside of a ganglion cell's receptive field could inhibit responses to a grating moved within a cell's receptive field. They recorded from axon-bearing amacrine cells and showed that they depolarized at times when action potentials were inhibited in ganglion cells recorded simultaneously on a multi-electrode array.

These hypotheses of axon-bearing amacrine cell function rest on the assumption that the axons are output structures that transmit spikes across the retina. Here we test this assumption in several ways. We perform detailed measurements of the spatial receptive field of A1 amacrine cells using spot and annulus stimuli better suited to measure center-surround structure than the small spots and bars previously used, and compare the physiological receptive field to the morphological dendritic and axonal fields. We find that the A1 does respond to light stimuli beyond its dendritic field but we present pharmacological evidence that these responses originate from a surround mechanism not associated with the axons. We show that blocking A1 action potentials has no significant effect on receptive field properties, consistent with the axons carrying an output signal. In addition, we image light-evoked calcium transients in the axons of A1 cells and show that voltage gated sodium channels are necessary for a light induced axonal calcium increase, consistent with the hypothesis that action potentials propagate through the axonal arbor.

Materials and methods

Tissue preparation

Tissue was prepared as previously described (Dacey et al., 2000*b*). In brief, *Macaca nemestrina* or *fascicularis* retinas were obtained from the tissue distribution program of the Washington National Primate Research Center at the University of Washington. Under deep barbiturate anesthesia eyes were enucleated and hemisected to remove the anterior pole including the lens and vitreous humor. The retina, choroid, and pigment epithelium were dissected as a unit from the sclera. Radial cuts were made to flatten the retina and it was fixed to a recording chamber with poly-L-lysine, vitreal side up. The chamber was mounted in an upright microscope for receptive field studies or a two-photon microscope for imaging studies. The retina was superfused with oxygenated Ames medium and maintained at 36°C. Pharmacological agents were mixed with Ames medium and applied to the bath superfusion. All pharmacological agents were obtained from Sigma (St. Louis, MO).

Electrical recording

Glass microelectrodes (R = 250–500 MΩ) were filled with 2% Neurobiotin and 2% pyranine in 1 M KCl. Retinal somata were stained with the vital dye acridine orange (several drops of 50 μM solution were added to the bath) and visualized with fluorescence episcopic illumination simultaneously with the microelectrode. A1 amacrine cell bodies were targeted based on their large (15–20 μm), round somas located in the center of the IPL or in the INL, and identity was confirmed after iontophoresis of pyranine allowed the examination of dendritic morphology *in vitro*. The electrode tip was positioned next to the soma and penetration was achieved using the amplifier's buzz feature. Intracellular voltage was amplified (Axoprobe 2B, Axon Instruments, Sunnyvale, CA) and digitized at 10 KHz. Data acquisition was controlled by custom software.

Tissue processing

Retinas were processed to recover the morphology of cells filled with Neurobiotin. At the end of the experiment retinas were dissected from the pigment epithelium and choroid, fixed in 4% paraformaldehyde in 0.1 M phosphate buffer for 2 h, rinsed overnight, and placed in a buffered solution of 0.1% Triton X-100 containing avidin-biotin-horseradish-peroxidase complexes (Vector Laboratories, Burlingam, CA) for 8 h. Retinas were then rinsed overnight, and horseradish-peroxidase histochemistry was performed with the use of diaminobenzidine (Kirkegaard & Perry Laboratories, Gaithersberg, MD) as the chromogen. Processed retinas were mounted on glass slides in a solution of polyvinyl alcohol and glycerol and stored at 4°C.

Visual stimuli

Visual stimuli were generated by a digital projector (Vista-GRAPHX 2500, Christie Digital, Cypress, CA) controlled by

custom software through a VSG3 stimulus generator (Cambridge Research Systems, England; Packer et al., 2001). Stimuli were focused through a 4× objective onto the retina. The retinal area covered by the stimulus was 2.96 × 2.22 mm. All stimuli used for receptive field measurements were white spots and annuli centered over the cell's receptive field, which were modulated above and below a mid-photopic background luminance (L_{BKG}, estimated photon flux = 3.4×10^5 photons/μm^2/s) at 100% contrast (contrast = L_{MAX}-L_{BKG}/L_{BKG}) at 2.03 Hz. A small test flash was first used to center the stimulus over the receptive field by manually moving it to elicit a maximum response. Twenty-four light flashes were presented to the cell and the responses were averaged and quantified by taking the maximum amplitude or the area of the ON and OFF components of the voltage response separately or averaged together. Statistical significance was determined by performing a Student *t*-test, with a *p* value of <0.05 indicating significance.

Calcium imaging

Retinas were mounted on a custom-built two-photon microscope (Denk et al., 1990). Fluorescence was excited by a mode-locked Ti:S laser, and emission was band pass filtered (535 ± 25 nm) and monitored with a photomultiplier tube. Electrodes were filled with 5 mM Oregon Green BAPTA-1 (OGB-1, Invitrogen, Carlsbad, CA) in 1 M KAcetate. Cells were labeled with acridine orange, and recordings obtained as described previously. Cells were allowed to fill with OGB for 30 to 90 min with negative current (50–100 pA) applied to the electrode because of the long time necessary to fill the axons, in some, but not all cells the electrical recording deteriorated by the time the axons were filled. In these cases the electrode was pulled off of the cell and it was allowed to recover for 30 to 60 min before imaging. Axons were easily identified by their extension > 500 μm from the soma. Fluorescence was collected in line scan mode at 2 ms/line. During imaging A1 cells were stimulated by a red LED (630 nm, 10 cd @ 20 mA, 15° viewing angle) that was placed above the retina and provided diffuse illumination. Responses to the LED were similar to responses to the digital projector used for receptive field studies. Raw fluorescence data was background-subtracted and the stimulus-evoked change in fluorescence intensity [F(t)] was scaled by the pre-stimulus intensity [F(0)] to give the ratio ΔF/F [$\Delta F/F = F(t) - F(0)/F(0)$]. Custom software controlled and coordinated imaging and physiological data collection. Morphological reconstructions of cells were obtained by taking image z-stacks at different positions, collapsing them and manually aligning the resulting tiles into a montage using ImageJ (NIH, rsb.info.nih.gov/ij).

Results

A1 center-surround receptive field structure

Primate cone bipolar cells have center-surround receptive field structure (Dacey et al., 2000*a*). ON cone bipolar cells have an ON center response that is antagonized by simultaneous surround stimulation. When stimulated in isolation, the surround produces and OFF response. The opposite is true for an OFF cone bipolar cell. With dendrites in ON and OFF sublamina of the IPL, A1 amacrine cells can receive input from both ON and OFF bipolar cells and should thus inherit centers and surrounds of both types. In previous receptive field studies using small spots and bars of light, an antagonistic surround was found in some rabbit polyaxonal amacrine cells (Volgyi et al., 2001), but not in primate A1 amacrine cells (Stafford & Dacey, 1997). However, these small stimuli are not ideally suited to measure center-surround interactions because of the large size and low gain of the surround. To further test for the presence of an antagonistic surround linked to the ON and/or OFF responses in A1 cells, the spatial receptive field was mapped using spot and annular stimuli.

Fig. 2A shows an example of A1 cell responses to spots of light at several diameters. The response to a 2000 μm spot (bottom) is smaller than the response to a 450 μm spot (middle), indicating the presence of an antagonistic surround. Fig. 2B shows the peak ON and OFF response amplitude as a function of spot diameter. As spot diameter increases the response reaches a maximum, after which the peak voltage decreases to 0.82 ± 0.03 (ON) and 0.78 ± .02 (OFF) of its maximum ($n = 28$). Fig. 2C shows the area under the voltage response as a function of spot diameter. As spot diameter increases the area reaches a maximum, after which it decreases to 0.46 ± 0.04 (ON) and 0.439 ± 0.04 (OFF) of its maximum ($n = 28$). The more substantial surround antagonism as measured by response area suggests that the surround's primary effect is to make the response more transient. As an estimate of the center size, we measured the spot size that elicited the maximum response area (494 ± 68 μm (ON) and 472 ± 64 μm (OFF), $n = 28$), which is approximately the size of the A1 dendritic tree diameter as previously reported [300–500 μm in the periphery (Dacey, 1989)].

To examine the surround in isolation we presented A1 cells with annuli. Fig. 2D shows the response of an A1 cell to several annuli with fixed outer diameters of 2000 μm and increasing inner diameters. The cells respond to surround stimulation at light onset and offset. At larger annulus inner diameters, the response consists of a fast component and a delayed component. The delayed component, which was not always obvious, could be due to delayed input from the surround, electrical coupling to neighboring A1 cells, or complex interactions of the ON and OFF systems. Fig. 2E shows the peak response of the ON and OFF components as a function of annulus inner diameter. The response initially decreases as center stimulation is removed. As the inner diameter increases further the response increases, because the center no longer antagonizes the surround and the surround dominates. The response then decreases because the surround is less stimulated, but it was still measurable even with annulus inner diameters of 1200 μm and occasionally 1800 μm. Fig. 2F shows the response area as a function of annulus inner diameter. The shape of the curve is similar, but because the surround is more evident in the area measurement, the initial decrease and increase are more exaggerated. As an arbitrary estimate of surround size we measured the point at which the annulus response function decreased to 50% of its maximum [675 ± 56 μm (ON) and 772 ± 57 (OFF), $n = 27$].

These results show that the A1 receptive field center consists of ON and OFF components, both of which are antagonized by surround stimulation. When stimulated in isolation, the surround produces ON and OFF responses. This could mean that the A1 receives input from ON and OFF bipolar cells, with OFF and ON surrounds, respectively.

Effect of L-AP4 on A1 receptive field

To further examine the retinal pathways that generate the ON and OFF responses of the center and surround, the receptive field properties of A1 cells were studied in the presence of L-(+)-2-Amino-4-phosphono-butyric acid (L-AP4), a compound that blocks

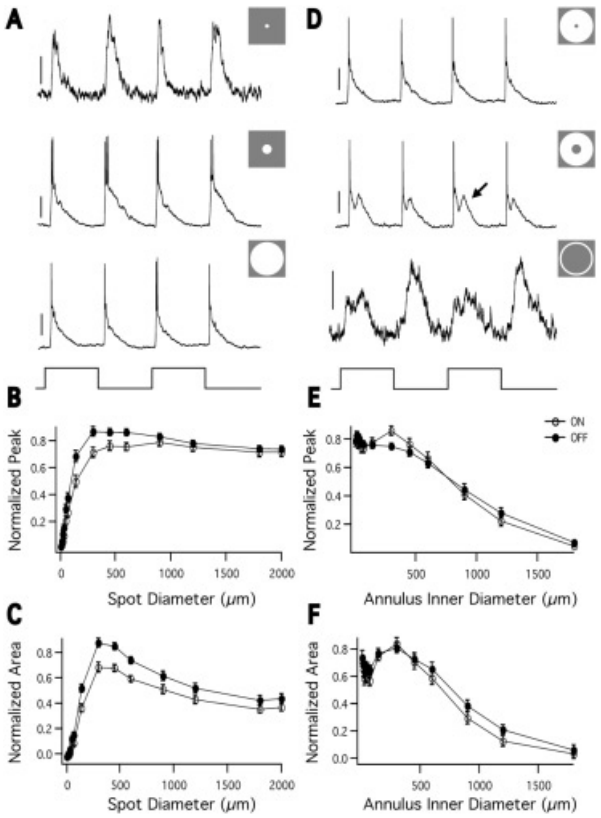

Fig. 2. A1 spatial receptive field probed with spots and annuli. **A**: Responses to 72 (top), 450 (middle), and 2000 (bottom) μm spots of light (stimulus trace below). All stimuli, unless otherwise noted, are flashed on and off at 250 ms intervals. Top scale bar = 4 mV, middle and bottom scale bars = 20 mV. **B**: The peak voltage response of the ON (open circles) and OFF (closed circles) components normalized to the maximum response amplitude, plotted against spot diameter, $n = 28$ cells. Error bars in this and all figures represent the standard error of the mean (SEM). As spot size increases, the response amplitude increases to a maximum, after which it decreases, indicating the presence of an inhibitory surround. **C**: The area of the voltage response of the ON (open circles) and OFF (closed circles) responses normalized to the maximum response area, plotted against spot diameter (the area response function). The ON and OFF components have similar area response functions. The surround is more evident than in the peak voltage measurements, $n = 28$. **D**: Responses to an annulus with 2000 μm outer diameter and 72 (top), 300 (middle), and 1200 (bottom) μm inner diameter (stimulus trace below). The 300 μm inner diameter annulus evokes fast and delayed (arrow) components. Top and middle scale bars = 20 mV, bottom scale bar = 4 mV. **E**: The peak voltage of the ON (open circles) and OFF (closed circles) responses normalized to the maximum response amplitude and plotted against annulus inner diameter. The outer diameter of the annulus was fixed at 2 mm. With small annulus inner diameter the center and surround antagonize each other to produce a diminished response. As the annulus inner diameter grows, the center is no longer stimulated and the surround is fully stimulated, yielding a larger response. As the annulus inner diameter grows further, the surround is stimulated less and the response decreases. $n = 27$. **F**: The area of the of the ON (open circles) and OFF (closed circles) voltage responses normalized to the maximum area and plotted against annulus inner diameter (the annulus response function). $n = 27$.

the ON pathway (Slaughter & Miller, 1981). If the A1 is inheriting its surround from bipolar cells, abolishing ON bipolar cell input with L-AP4 should abolish the ON center and OFF surround and leave the OFF center and ON surround inherited from the OFF bipolar cell intact. In the presence of 100 μM L-AP4, spots of light evoke a normal OFF response and no ON response at all spot sizes (Figs. 3A, 3B). This is consistent with ON bipolar cell input generating ON center responses.

The OFF responses to spots up to ~ 300-μm are not affected by L-AP4. Blocking the ON pathway does, however, weaken the antagonism of the OFF response by larger diameter spots (Fig. 3C). The OFF response to a 2000 micron spot is 0.36 ± 0.03 of

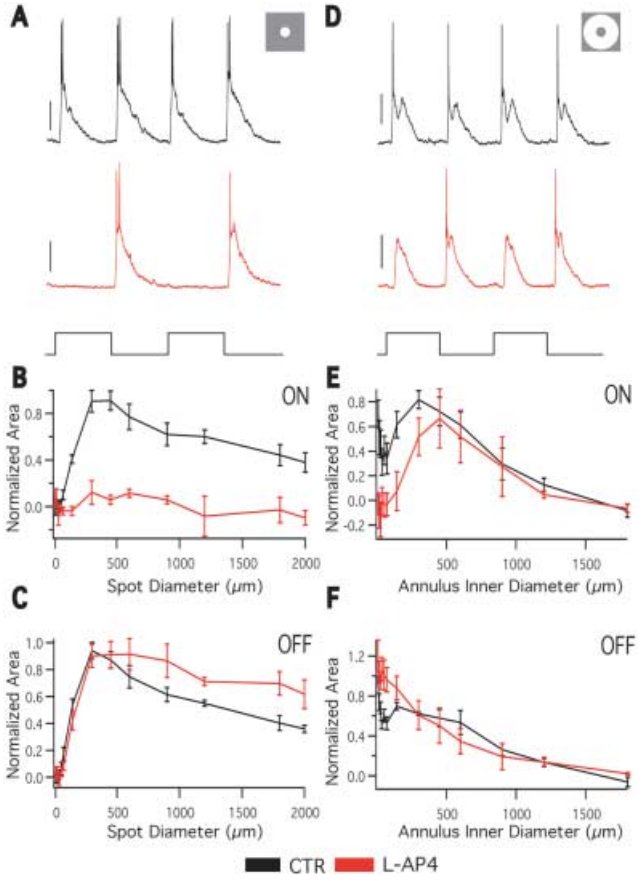

Fig. 3. Effect of L-AP4 on A1 receptive field. A: Responses to a 300 μm spot in the absence (black) and presence (red) of 100 μM L-AP4 (stimulus below traces). L-AP4 eliminates the ON component of the spot response, but the OFF component is unchanged. **B**: The area response function of the ON component of the light response in the absence (black) and presence (red) of L-AP4. L-AP4 eliminates the ON response at all spot sizes. $n = 4$. **C**: The area response function of the OFF component of the light response in the absence (black) and presence (red) of L-AP4. In the presence of L-AP4 The OFF response to large spots is increased, indicating a decrease of surround antagonism. $n = 4$. **D**: Responses to a 450 μm inner diameter annulus in the absence (black) and presence (red) of L-AP4 (stimulus trace below). In response to the annulus, both ON and OFF responses are evoked in the presence of L-AP4. Scale bars = 20 mV. **E**: The annulus response function of the ON component of the light response in the absence (black) and presence (red) of L-AP4. As the annulus inner diameter grows, the ON response returns to control levels, indicating it originates from the OFF system. $n = 4$. **F**: The annulus response function of the OFF component of the light response in the absence (black) and presence (red) of L-AP4. The OFF response is elevated at small annulus inner diameters, indicating a decrease of surround antagonism. At larger annulus inner diameters, the OFF response is the same as control, indicating the OFF surround response originates from the OFF pathway. $n = 4$.

maximum in control and 0.61 ± 0.07 of maximum in the presence of L-AP4 ($p = 0.012$, $n = 5$). This indicates that OFF bipolar cell input generates the OFF center response, but that these responses are antagonized in part by a surround mechanism generated by the ON pathway.

L-AP4 blocks ON responses evoked by annuli with small but not large inner diameters (Figs. 3D, 3E). This is consistent with the A1 inheriting its ON surround from OFF bipolar cell input. Annuli with small inner diameters evoke no response because the OFF center and ON surround of the OFF bipolar cells antagonize each other.

L-AP4 increased OFF responses to annuli with small inner diameters (Fig. 3F), consistent with the decreased surround antagonism observed in response to large spots (Fig. 3C). However, OFF responses evoked by annuli with large inner diameters were not significantly affected by L-AP4. This is surprising, because it means the A1 does not receive its OFF surround responses from ON bipolar cell input, and it also indicates that some other mechanism that is maintained in the presence of L-AP4 generates OFF surround responses. One possibility is that neighboring A1 cells, which show extensive tracer coupling (Dacey, 1989; Wright & Vaney, 2004), could pass their OFF center responses to the recorded cell *via* electric coupling. These response would appear as OFF surround responses.

Overall, these data are consistent with bipolar cell input being responsible for the A1 cell center-surround receptive field structure but do not support a pure separation of the ON and OFF pathways. The ON pathway appears to contribute some surround antagonism of the OFF center response, and the OFF pathway appears to contribute to OFF surround responses.

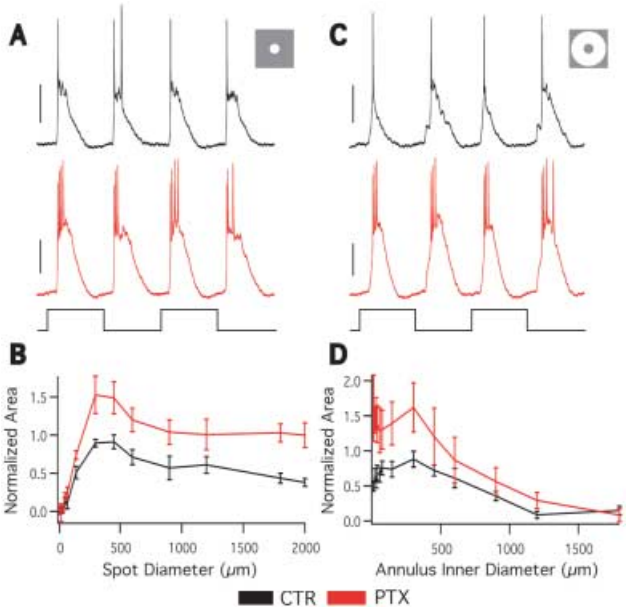

Fig. 4. Effect of picrotoxin on A1 receptive field. **A**: Responses to a 450 μm spot in the absence (black) and presence (red) of 100-μM PTX (stimulus trace below). The picrotoxin response is larger than control. Scale bars = 10 mV. **B**: The averaged area response function in the absence (black) and presence (red) of PTX. PTX increases the response at all spot sizes, but surround antagonism is still present. n = 4. **C**: Responses to a 450 μm inner diameter annulus in the absence (black) and presence (red) of PTX (stimulus trace below). Scale bars = 20 mV. **D**: The averaged annulus response function in the absence (black) and presence (red) of PTX. PTX increases the response at all annulus sizes, though the increase is predominantly at small annulus inner diameters. $n = 4$.

Effect of picrotoxin on A1 receptive field

To test what role GABAergic inhibition plays in the A1 amacrine cell receptive field, specifically in the generation of the A1 antagonistic surround, we mapped the spatial receptive field in the presence of 100-μM picrotoxin (PTX) that blocks GABA A and C receptors. PTX increased the response amplitude at all spot (Figs. 4A, 4B) and annulus (Figs. 4C, 4D) sizes. However, the center size, surround size, and surround antagonism were not significantly affected by PTX (Table 1). These results indicate that GABAergic inhibition participates in the retinal circuitry of the A1 cell, but it is not involved in surround antagonism.

Effect of tetrodotoxin on A1 receptive field

To test the hypothesis that action potentials serve an output function in A1 cells, we mapped the spatial receptive field in the presence of 0.5 μM tetrodotoxin (TTX), which blocks the voltage gated sodium channels responsible for fast action potential generation. If action potentials are purely an output signal that propagates away from the soma, then TTX should not affect the receptive field size measurements. However, if the action potentials serve to propagate input to the soma along the axons, TTX should reduce the spatial receptive field size by eliminating responses that originate outside the dendritic field. Application of TTX completely abolished A1 fast action potentials, but it had little effect on depolarizations (Figs. 5A, 5C) or the receptive field properties (Figs. 5B, 5D). Center size, surround size, and surround antagonism were not significantly affected by TTX (Table 1). These results indicate TTX sensitive sodium channels are not involved in the generation of the light response in A1 cells and are inconsistent with action potentials propagating inputs to the cell from beyond the dendritic field *via* the axons.

Calcium imaging of A1 axons and dendrites

We used two-photon imaging to directly measure light-evoked calcium changes in the axons and dendrites of A1 cells. Two-photon imaging allows the excitation of fluorophores in the retina with minimal excitation of photoreceptors, because the excitation source is an infrared laser and two-photon excitation of the fluorophore is restricted to the laser's focal point (Denk & Detwiler,

Table 1. *Effect of PTX and TTX on A1 receptive field properties*

	Center Size (μm)	Surround Size (μm)	Surround Strength
CTR	413 ± 38	678 ± 94	0.34 ± 0.1
PTX	338 ± 38	646 ± 138	0.65 ± 0.1
p ($n = 4$)	0.18	0.818	0.068
CTR	420 ± 56	599 ± 134	0.58 ± 0.06
TTX	540 ± 102	560 ± 134	0.74 ± 0.06
p ($n = 5$)	0.1	0.41	0.18

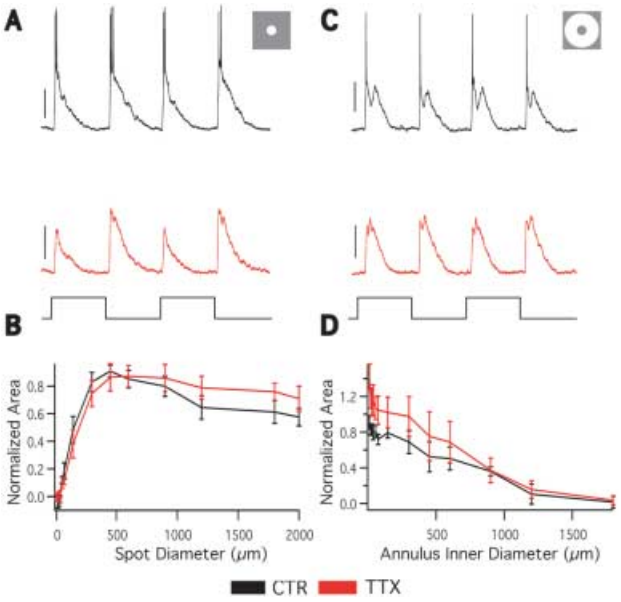

Fig. 5. Effect of tetrodotoxin on A1 receptive field. **A**: Responses to a 450 μm spot of light in the absence (black and presence (red) of 0.5 μM TTX (stimulus trace below). TTX eliminates the action potentials but minimally effects light-evoked depolarizations. Scale bars = 20 mV. **B**: The average area response function in the absence (black) and presence (red) of TTX. TTX. n = 5. **C**: Responses to a 450 μm inner diameter annulus in the absence (black) and presence (red) of TTX (stimulus trace below). Scale bars = 20 mV. **D**: The averaged annulus response function in the absence (black) and presence (red) of TTX. The responses in the surround are similar with and without TTX. n = 5.

1999; Euler et al., 2002). Cells were filled with the calcium sensitive dye OGB-1 through the recording electrode (Figs. 1A, 6A). We could unambiguously identify processes as axons by their small diameter, lack of spines, sparse branching, and extension

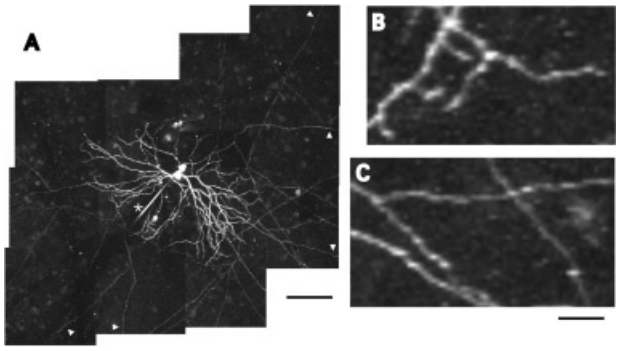

Fig. 6. Oregon green filled A1 cell. **A**: An A1 amacrine cell filled with the calcium sensitive dye Oregon Green Bapta-1 and imaged on a two-photon microscope. The image is a reconstruction from several higher magnification images, each of which were compressions of image stacks in the z dimension. Thin axons are clearly seen extending beyond the restricted dendritic field (arrowheads). The recording electrode is marked with an asterisk. Scale bar = 100 μm. **B**: High magnification view of A1 dendrites. The dendrites are thick, moderately branched, and have spine-like protrusions. Scale bar = 20 μm. **C**: High magnification view of A1 axons. The axons are thin, sparsely branched and have bouton-like swellings. Scale bar = 20 μm.

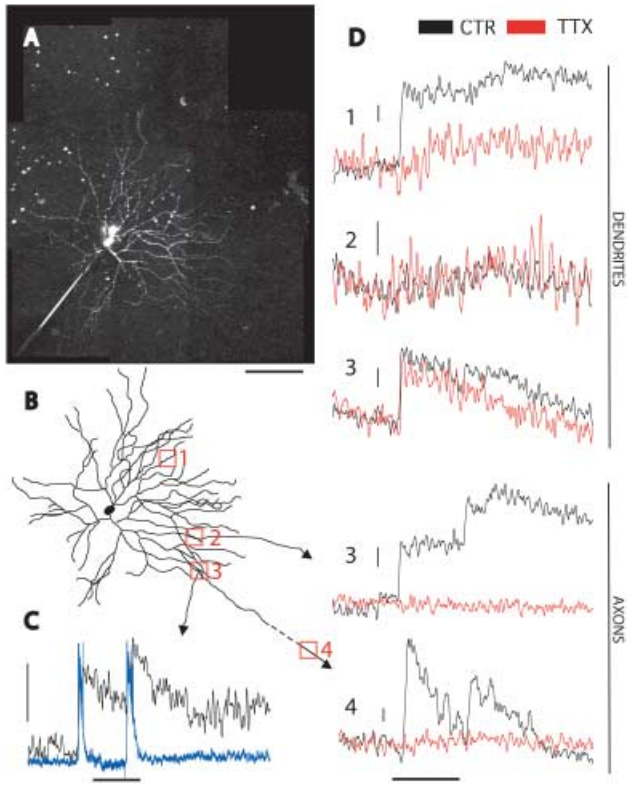

Fig. 7. Calcium imaging in A1 axons and dendrites. **A**: An A1 cell filled with OGB-1 imaged with a two-photon microscope. The image is a reconstruction from several higher magnification images, each of which were compressions of image stacks in the z dimension. The axonal arbor was not completely filled, and the axons are very thin and dim, but several were traced as far as 600 μm from the soma. Scale bar = 100 μm. **B**: A tracing of the cell in A. The filled axons have arrowheads. The red numbered boxes indicate locations of linescans in D. Location 4 is beyond the scale of the image, 608 μm from the soma. **C**: Simultaneous electrical (blue) and optical (black) recording from an A1 cell showing the response to a 1 s flash of a red LED (stimulus bar below traces). The vertical scale bar represents 15 mV and 20% fluorescence change ($\Delta F/F$) (This recording was from the cell pictured in Fig. 1A). **D**: Linescans from locations in B in response to a 1 s red LED flash (stimulus bar at bottom) in the absence (black) and presence (red) of 0.5 μM TTX. The top three traces are from dendrites, and the bottom two axons. In location 3 a dendrite and axon were imaged simultaneously. Location 4 was beyond the scale of the image in B, 608 μm from the soma. The dendritic locations showed variable light induced fluorescence changes (location 2 had no change) and variable effect of TTX (location 1 was much more affected than location 3). The axonal fluorescence changes were always present and always completely abolished by TTX. Vertical scale bars represent 10% $\Delta F/F$.

>500 μm from the soma (Fig. 6C). Dendrites, conversely, were thicker, had spines, branched extensively, and did not extend long distances from the soma (Fig. 6B). Seven cells were filled with OGB. Five of those were filled sufficiently to image axons. We observed light-induced fluorescence changes in each of seven axonal locations from those five cells. The dendritic calcium change was variable. Two of seven cells had no light-induced fluorescence changes at any dendritic location imaged. The remaining five cells had light-induced fluorescence changes at all dendritic locations imaged, except one (Fig. 7D, location 2). In axonal and dendritic locations fluorescence changes occurred at

light onset and offset, coincident with light induced depolarizations (Fig. 7C). We then tested the effect of TTX application on calcium transients in both dendrites and axons. If the dendrites are input structures and the axons output structures, with action potentials propagating along the axons, then the calcium change observed in the axons should be blocked by TTX, which blocks action potentials. The calcium change in the dendrites, if independent of action potential propagation, should persist in the presence of TTX. After application of TTX, the calcium change in the axon was completely abolished in all cases (Fig. 7D, locations 3 and 4). The fluorescence change in TTX was 0.00 ± 0.019 of control, ($n = 7$ locations from five cells). By contrast the effect of TTX on dendrites was variable. In some cases there was little effect (Fig. 7D, location 3), and in some other cases there was a more substantial effect (Fig. 7D, location 1). In the presence of TTX, the dendritic fluorescence change was decreased to 0.34 ± 0.09 ($n = 9$ locations from five cells) of control, but not abolished. These results suggest that action potentials are required for an axonal but not dendritic calcium change.

Discussion

We have shown that A1 cells have antagonistic center-surround receptive field organization in both the ON and OFF fields. A1 surrounds are larger than those of ganglion cells but TTX does not affect the basic center-surround receptive field structure, so we conclude that action potentials do not contribute to the A1 center or large surround. We have also shown that TTX abolishes a light-induced calcium transient in A1 axons, but not in dendrites. Together, we interpret these results as supporting the hypothesis that A1 action potentials are generated in proximal axons and propagate away from the soma across the retina.

Receptive field organization

Our results are largely consistent with the A1 amacrine cell building its center-surround receptive field by combining inputs from ON bipolar cells with OFF surrounds and OFF bipolar cells with ON surrounds. Consistent with this interpretation, primate diffuse bipolar cells have center-surround receptive fields (Dacey et al., 2000*a*). Our results with L-AP4, however, are inconsistent with a complete separation of the ON and OFF pathways. L-AP4 does not block OFF surround responses in A1 cells, which would be expected if they originated in the ON bipolar cell pathway. This could reflect the influence of electric coupling to neighboring A1 cells, whose OFF center responses are not blocked by L-AP4. The Gaussian receptive field surround diameters (the diameter at which a Gaussian receptive field fit decreases to 1/e of its maximum) of diffuse cone bipolar cells in peripheral primate retina are ~750 μm. Parasol ganglion cells, which have dendritic field sizes similar to the A1 cell, are believed to inherit their surrounds from bipolar cell input (McMahon et al., 2004) and have Gaussian surround diameters similar to those of diffuse bipolar cells (Croner & Kaplan, 1995). As a comparison the A1 annulus response decreases to 1/e of its maximum at ~925 μm. The larger surround of A1 cells is inconsistent with its surround being generated purely from bipolar cell input. Coupling could also play a role in generating the large surrounds of A1 cells.

The A1 cell's antagonistic surround extends beyond its dendritic arbor. Surround responses could arise from input to the axonal arbor but several pieces of evidence argue against this. The amplitude of responses outside the dendritic arbor decreases to 50% within 760 μm. This surround size is slightly larger than a typical ganglion cell's surround but much smaller than the A1 axonal arbor. Responses from beyond the dendritic arbor are unchanged after application of TTX, which suggests that action potentials propagating along the axons are not involved in inputs originating outside the dendritic arbor. If the antagonistic surround were generated by inhibitory GABAergic input to the axons, then PTX would block the surround; but it does not. Together, these results are consistent with an axon-independent surround mechanism.

Parasol ganglion cell surrounds are believed to be generated in the outer retina by GABA independent horizontal cell feedback, because surround antagonism is insensitive to PTX and TTX, which should affect inner retinal mechanisms of lateral inhibition (McMahon et al., 2004). Surround antagonism in A1 amacrine cells is not significantly changed in the presence of PTX and TTX, suggesting that like parasol cells, an outer retinal mechanism involving horizontal cell feedback is primarily responsible for generating the antagonistic surround. Further pharmacological experiments examining the effect of drugs believed to affect horizontal cell feedback, such as Co^{2+}, HEPES, and carbenoxelone (Hirasawa & Kaneko, 2003; Kamermans et al., 2001; McMahon et al., 2004; Vessey et al., 2005; Vigh & Witkovsky, 1999) will help resolve the specific contributions of outer retinal feedback to the A1 surround.

PTX does have a significant effect on the light responses of A1 cells, substantially increasing their amplitude. GABAergic inhibition thus appears to have a role in A1 circuitry independent of surround antagonism. PTX would block any direct GABAergic inputs to A1 cells but would also disinhibit other cells that receive GABAergic inhibition, and that could interact with the A1 cell, for example glycinergic amacrine cells.

Light evoked calcium transients

The calcium response in A1 axons is completely abolished by TTX, indicating a necessity of voltage-gated sodium channels. We interpret this as meaning the action potentials recorded in the soma of A1 cells propagate along the axons. The observed calcium influx is probably caused by the opening of voltage gated calcium channels caused by action potential propagation and depolarization. The A1 axons have swellings along their length that resemble presynaptic boutons. If these are in fact presynaptic structures, the presence of voltage gated calcium channels could serve to couple depolarization to vesicular neurotransmitter release. We also observe calcium changes in non-swelling locations. It is possible that there are presynaptic structures throughout the axons, or that calcium channels are present throughout the axons, independent of other presynaptic elements. Calcium increases in response to action potentials have been observed in myelinated axons of rat and mouse optic nerve (Lev-Ram & Grinvald, 1987; Zhang et al., 2006) but not in the unmyelinated intra-retinal portion of mouse ganglion cell axons (unpublished observation, D.J. Margolis, A.J. Gartland, and P.B. Detwiler). Because there are no presynaptic elements in the myelinated axon, the action potential evoked calcium signals are believed to play a role in processes other than initiation of vesicular release (e.g., in coupling activity to energy metabolism) (Zhang et al., 2006), which raises the possibility that the calcium increases in A1 axons participate in similar non-synaptic events, in addition to or instead of playing a role in synaptic output.

The dendritic calcium change is heterogeneous. There were locations at which we observe no light-induced calcium change.

The variability of the light-induced calcium increase at a specific dendritic location could be caused by several factors, including the proximity to synaptic inputs, the local distribution and concentration of voltage gated calcium channels, the affect of action potential back propagation, and the contribution of calcium release from internal stores. When we do observe a dendritic calcium change it is diminished but not abolished by TTX. This effect of TTX could be caused by dendritic sodium channels providing some boosting of the postsynaptic depolarization (Oesch et al., 2005) or it could be because of back-propagation of action potentials from the soma/axons. We favor the back-propagation explanation, because TTX does not have a substantial effect on the sub-spike voltage responses recorded at the soma. Therefore voltage-gated sodium channels do not seem to play an important role in integrating or boosting synaptic inputs and generating those responses. There are also examples from other cell types of a similar abatement of dendritic calcium increases after TTX application (Goldberg et al., 2003; Oesch et al., 2005) attributable to action potential back-propagation. In the context of action potential back-propagation, the variable effect of TTX on the dendritic calcium transients could be because of a variability of locations imaged relative to axonal origins where spikes are presumably initiated. We did not observe a dependence on distance from the soma of dendritic calcium changes (data not shown), but a more thorough and systematic sampling of dendritic tree locations will be needed to address this possibility.

Comparison to previous studies

A1 cell receptive field sizes previously reported were slightly larger than what we report here, and were on average ~ 1.5 times the dendritic field size (Stafford & Dacey, 1997). This can be reconciled with our results in that the large receptive fields probably reflect the surround generating ON-OFF responses that are not readily distinguishable from center responses, as measured with small spot and bar stimuli not ideal for studying center-surround interactions. Volgyi et al. (2001) studied the receptive field properties of six classes of polyaxonal amacrine cells in rabbit retina. They also found a correspondence of dendritic and receptive field sizes. Their PA1 cell, which they believed most analogous to the primate A1 cell, has a weakly inhibitory surround as measured by peak response amplitudes. This is in agreement with the A1 surround having an effect primarily on the area of the response, not the peak voltage. Receptive fields larger than dendritic fields have been used as an argument that axons could be providing input to axon-bearing amacrine cells (Freed et al., 1996). This may be a misinterpretation based on a failure to appreciate the influence of the surround.

Bloomfield (1996) found that TTX had no effect on the receptive field size of rabbit amacrine cells with dendritic fields $< 525\ \mu$m, but that it decreased receptive field size in cells with larger dendritic fields, suggesting that action potentials were required to propagate information across large dendritic arbors. He also found good agreement between amacrine dendritic and receptive fields. Primate A1 amacrines have dendritic fields mostly smaller than 525 μm, and both the relation of dendritic to receptive field size, and the minimal effect of TTX on receptive field size are in agreement with Bloomfield's results.

A1 cell circuitry

Our study provides insight into the light response properties of A1 amacrine cells and provides new evidence that the axons function as spiking output structures. It will be important in future work to determine the synaptic targets of the A1 cells and whether the dendrites are postsynaptic and axons presynaptic as the physiology predicts. Primate magnocellular-pathway ganglion cells have recently been shown to be influenced by stimuli outside their classical receptive field (Solomon et al., 2006). Another possible target for the A1 is an ON-OFF "broad thorny" ganglion cell type that co-stratifies with the A1 dendritic and axonal fields in the middle of the IPL, has an ON-OFF transient light response, and projects to the LGN and superior colliculus (Dacey et al., 2003). It is likely that the A1 cells are GABAergic (Mariani et al., 1987). If the A1 cell axons selectively contact the broad thorny cell it could provide long-range inhibition from beyond the ganglion cells receptive field. This hypothesis could be explored by determining the degree to which the broad thorny cell, as well as other ganglion cell types in macaque retina, is strongly inhibited by global motion outside its receptive field.

The initial description of the A1 amacrine cell (Dacey, 1989) led to the postulate that the extensive network of axons operated as a unit, performing a global retinal function. More recent studies (Olveczky et al., 2003; Roska & Werblin, 2003) have provided some evidence that they are involved in inhibition in response to global image motion. Our results strengthen the overall hypothesis that the macaque A1 cell axons are spiking output structures and may serve as key elements for long-range lateral inhibition in the retina.

Acknowledgments

This work was funded by NIH grants EY02048 (PBD), EY06678 (DMD), EY01730 (Vision Research Center), RR00166 (Tissue Distribution Program of the Washington National Primate Research Center), GM07108 (CMD), and the Paul Kayser International Award in Retinal Research from the Retina Research Foundation (DMD). The authors thank Orin Packer, Julian Vrieslander, Toni Haun, and Beth Peterson for programming and technical assistance, Winfried Denk for providing custom parts and directions for assembling our 2-photon microscope, and Thomas Euler for helpful comments on this manuscript.

References

Bloomfield, S.A. (1996). Effect of spike blockade on the receptive-field size of amacrine and ganglion cells in the rabbit retina. *Journal of Neurophysiology* **75**, 1878–1893.

Croner, L.J. & Kaplan, E. (1995). Receptive fields of P and M ganglion cells across the primate retina. *Vision Research* **35**, 7–24.

Dacey, D., Packer, O.S., Diller, L., Brainard, D., Peterson, B. & Lee, B. (2000*a*). Center surround receptive field structure of cone bipolar cells in primate retina. *Vision Research* **40**, 1801–1811.

Dacey, D.M. (1988). Dopamine-accumulating retinal neurons revealed by in vitro fluorescence display a unique morphology. *Science* **240**, 1196–1198.

Dacey, D.M. (1989). Axon-bearing amacrine cells of the macaque monkey retina. *Journal of Comparative Neurology* **284**, 275–293.

Dacey, D.M. (1990). The dopaminergic amacrine cell. *Journal of Comparative Neurology* **301**, 461–489.

Dacey, D.M., Diller, L.C., Verweij, J. & Williams, D.R. (2000*b*). Physiology of L- and M-cone inputs to H1 horizontal cells in the primate retina. *Journal of the Optical Society of America A: Optics Image Science and Vision* **17**, 589–596.

Dacey, D.M., Peterson, B.B., Robinson, F.R. & Gamlin, P.D. (2003). Fireworks in the primate retina: In Vitro photodynamics reveals diverse LGN-projecting ganglion cell types. *Neuron* **37**, 15.

Denk, W. & Detwiler, P.B. (1999). Optical recording of light-evoked calcium signals in the functionally intact retina. *Proceedings of the National Academy of Sciences* **96**, 7035–7040.

Denk, W., Strickler, J.H. & Webb, W.W. (1990). Two-photon laser scanning fluorescence microscopy. *Science* **248**, 73.

Euler, T., Detwiler, P.B. & Denk, W. (2002). Directionally selective calcium signals in dendrites of starburst amacrine cells. *Nature* **418**, 845–852.

Famiglietti, E.V. (1992*a*). Polyaxonal amacrine cells of rabbit retina: morphology and stratification of PA1 cells. *Journal of Comparative Neurology* **316**, 391–405.

Famiglietti, E.V. (1992*b*). Polyaxonal amacrine cells of rabbit retina: PA2, PA3, and PA4 cells. Light and electron microscopic studies with a functional interpretation. *Journal of Comparative Neurology* **316**, 422–446.

Famiglietti, E.V. (1992*c*). Polyaxonal amacrine cells of rabbit retina: Size and distribution of PA1 cells. *Journal of Comparative Neurology* **316**, 406–421.

Freed, M.A., Pflug, R., Kolb, H. & Nelson, R. (1996). ON-OFF amacrine cells in cat retina. *Journal of Comparative Neurology* **364**, 556–566.

Goldberg, J.H., Tamas, G. & Yuste, R. (2003). Ca2+ imaging of mouse neocortical interneurone dendrites: Ia-type K+ channels control action potential backpropagation. *Journal of Physiology* **551**, 49–65.

Hirasawa, H. & Kaneko, A. (2003). pH Changes in the invaginating synaptic cleft mediate feedback from horizontal cells to cone photoreceptors by modulating Ca2+ channels. *Journal of General Physiology* **122**, 657–671.

Kamermans, M., Fahrenfort, I., Schultz, K., Janssen-Bienhold, U., Sjoerdsma, T. & Weiler, R. (2001). Hemichannel-mediated inhibition in the outer retina. *Science* **292**, 1178–1180.

Kruger, J., Fischer, B. & Barth, R. (1975). The shift-effect in retinal ganglion cells of the rhesus monkey. *Experimental Brain Research* **23**, 443–446.

Lev-Ram, V. & Grinvald, A. (1987). Activity-dependent calcium transients in central nervous system myelinated axons revealed by the calcium indicator Fura-2. *Biophysical Journal* **52**, 571–576.

Mariani, A.P., Cosenza-Murphy, D. & Barker. J.L. (1987). GABAergic synapses and benzodiazepine receptors are not identically distributed in the primate retina. *Brain Research* **415**, 153–157.

McMahon, M.J., Packer, O.S. & Dacey, D.M. (2004). The classical receptive field surround of primate parasol ganglion cells is mediated primarily by a non-GABAergic pathway. *Journal of Neuroscience* **24**, 3736–3745.

Oesch, N., Euler, T. & Taylor, W.R. (2005). Direction-selective dendritic action potentials in rabbit retina. *Neuron* **47**, 739.

Olveczky, B.P., Baccus, S.A. & Meister, M. (2003). Segregation of object and background motion in the retina. *Nature* **423**, 401–408.

Packer, O., Diller, L.C., Verweij, J., Lee, B.B., Pokorny, J., Williams, D.R., Dacey, D.M. & Brainard, D.H. (2001). Characterization and use of a digital light projector for vision research. *Vision Research* **41**, 427.

Roska, B. & Werblin, F. (2003). Rapid global shifts in natural scenes block spiking in specific ganglion cell types. *Nature Neuroscience* **6**, 600–608.

Slaughter, M.M. & Miller, R.F. (1981). 2-amino-4-phosphonobutyric acid: A new pharmacological tool for retina research. *Science* **211**, 182–185.

Solomon, S.G., Lee, B.B. & Sun, H. (2006). Suppressive surrounds and contrast gain in magnocellular-pathway retinal ganglion cells of Macaque. *Journal of Neuroscience* **26**, 8715–8726.

Stafford, D.K. & Dacey, D.M. (1997). Physiology of the A1 amacrine: A spiking, axon-bearing interneuron of the macaque monkey retina. *Visual Neuroscience* **14**, 507–522.

Taylor, W.R. (1996). Response properties of long-range axon-bearing amacrine cells in the dark-adapted rabbit retina. *Visual Neuroscience* **13**, 599–604.

Vessey, J.P., Stratis, A.K., Daniels, B.A., Da Silva, N., Jonz, M.G., Lalonde, M.R., Baldridge, W.H. & Barnes, S. (2005). Proton-mediated feedback inhibition of presynaptic calcium channels at the cone photoreceptor synapse. *Journal of Neuroscience* **25**, 4108–4117.

Vigh, J. & Witkovsky, P. (1999). Sub-millimolar cobalt selectively inhibits the receptive field surround of retinal neurons. *Visual Neuroscience* **16**, 159–168.

Volgyi, B., Xin, D., Amarillo, Y. & Bloomfield, S.A. (2001). Morphology and physiology of the polyaxonal amacrine cells in the rabbit retina. *Journal of Comparative Neurology* **440**, 109–125.

Werblin, F.S. (1972). Lateral interactions at inner plexiform layer of vertebrate retina: Antagonistic responses to change. *Science* **175**, 1008–1010.

Witkovsky, P. (2004). Dopamine and retinal function. *Documenta Ophthalmologica* **108**, 17–40.

Wright, L.L. & Vaney, D.I. (2004). The type 1 polyaxonal amacrine cells of the rabbit retina: A tracer-coupling study. *Visual Neuroscience* **21**, 145–155.

Zhang, C-L., Wilson, J.A., Williams, J. & Chiu, S.Y. (2006). Action potentials induce uniform calcium influx in mammalian myelinated optic nerves. *Journal of Neurophysiology* **96**, 695–709.